JOURNAL OF THE AMERICAN CHEMICAL SOCIETY

Subscriber access provided by EDINBURGH UNIVERSITY LIBRARY | @ http://www.lib.ed.ac.uk

Communication

Construction of Fully Conjugated Covalent Organic Frameworks via Facile Linkage Conversion for Efficient Photoenzymatic Catalysis

Yuancheng Wang, Hui Liu, Qingyan Pan, Chenyu Wu, Wenbo
Hao, Jie Xu, Renzeng Chen, Jian Liu, Zhibo Li, and Yingjie Zhao

J. Am. Chem. Soc., **Just Accepted Manuscript** • DOI: 10.1021/jacs.0c00923 • Publication Date (Web): 12 Mar 2020

Downloaded from pubs.acs.org on March 12, 2020

Just Accepted

“Just Accepted” manuscripts have been peer-reviewed and accepted for publication. They are posted online prior to technical editing, formatting for publication and author proofing. The American Chemical Society provides “Just Accepted” as a service to the research community to expedite the dissemination of scientific material as soon as possible after acceptance. “Just Accepted” manuscripts appear in full in PDF format accompanied by an HTML abstract. “Just Accepted” manuscripts have been fully peer reviewed, but should not be considered the official version of record. They are citable by the Digital Object Identifier (DOI®). “Just Accepted” is an optional service offered to authors. Therefore, the “Just Accepted” Web site may not include all articles that will be published in the journal. After a manuscript is technically edited and formatted, it will be removed from the “Just Accepted” Web site and published as an ASAP article. Note that technical editing may introduce minor changes to the manuscript text and/or graphics which could affect content, and all legal disclaimers and ethical guidelines that apply to the journal pertain. ACS cannot be held responsible for errors or consequences arising from the use of information contained in these “Just Accepted” manuscripts.

is published by the American Chemical Society. 1155 Sixteenth Street N.W.,
Washington, DC 20036

Published by American Chemical Society. Copyright © American Chemical Society.
However, no copyright claim is made to original U.S. Government works, or works
produced by employees of any Commonwealth realm Crown government in the course
of their duties.

Construction of Fully Conjugated Covalent Organic Frameworks via Facile Linkage Conversion for Efficient Photoenzymatic Catalysis

Yuancheng Wang,†,+ Hui Liu,†,+ Qingyan Pan,† Chenyu Wu,† Wenbo Hao,† Jie Xu,† Renzeng Chen,† Jian Liu,‡ Zhibo Li,*,† and Yingjie Zhao*,†

†Key Laboratory of Biobased Polymer Materials, Shandong Provincial Education Department; College of Polymer Science and Engineering, Qingdao University of Science and Technology, Qingdao 266042, China

‡College of Materials Science and Engineering, Qingdao University of Science and Technology, Qingdao 266042, China

Supporting Information Placeholder

ABSTRACT: Covalent organic frameworks (COFs) with improved stability and extended π-conjugation structure are highly desirable. Here, two imine-linked COFs were converted into ultrastable and π-conjugated fused-aromatic thieno[3,2-c]pyridine-linked COFs (**B-COF-2** and **T-COF-2**). The successful conversion was confirmed by infrared and solid-state ^{13}C NMR spectroscopies. Furthermore, the structures of thieno[3,2-c]pyridine-linked COFs were evaluated by TEM and PXRD. It is noted that a slight difference in the structure leads to totally different photo-activity. The fully π-conjugated **T-COF-2** containing triazine as the core exhibited excellent photo-catalytic NADH regeneration yield of 74% in 10 min.

Covalent Organic Frameworks (COFs) are crystalline porous materials with precise structures. COFs have attracted considerable attention due to their unique structures. These features make COFs useful for application in gas storage and separation,[1-5] heterogeneous catalysis,[6-9] optoelectronics,[10-15] sensing,[16-19] energy storage,[20-21] etc. The basic principles to design and synthesize highly ordered structures lie in the reversible formation of covalent bonds. Until now, the mostly used linkages for constructing COFs are limited in B-O,[22-24] B-N,[25] Si-O[26-27] and C=N bond[28-29]. The self-adjusting property of these bonds can facilitate the formation of well-ordered structures. However, the chemical stability and conjugation are sacrificed due to the poor stability and weak electron delocalization of these bonds. Many efforts have been made to explore new chemistry to construct highly stable and electron delocalized COFs. Oxazole,[8, 30-32] thiazole,[31, 33] vinylene,[34-38] sp² carbon-carbon linkages (cyano-group-included),[39-42] β-hydroxyimine or hydroxylamine,[43] aryl-ether,[44] pyrazine,[45-46] dioxin,[47] imidazole[48] as novel linkages have been used in making ultrastable COFs. It is worth mentioning that some of the linkages mentioned above such as sp² carbon-carbon linkages could make fully π-conjugated COFs with ultrastability which broadens the application fields to organic electronics, supercapacitor, photo-catalysis, cathode for lithium-ion batteries, ferromagnetic materials and so on.[35, 38-39, 42, 45] Although the fully π-conjugated COFs is fascinating, to obtain crystallinity is still extremely difficult. The reversibility of the conjugated bond is usually bad which is unfavorable for the self-adjusting. Yaghi,[31] Liu,[49] Lotsch[33] and Baek[32] reported a two-steps post-synthetic strategy to convert the reversible imine bond into more stable and π-electron delocalized linkages such as thiazole, oxazole and quinolone. This is undoubtedly an easier and much more efficient way to achieve the aims of high crystallinity, improved electron delocalization and stability simultaneously as the highly ordered imine skeleton is already set at the first step. Herein, we report the synthesis of two ultrastable fully π-conjugated 2D COFs (**B-COF-2** and **T-COF-2**) linked by thieno[3,2-c]pyridine units achieved by a post-oxidative cyclization (Scheme 1). The basic chemistry for constructing the ordered skeleton is still Schiff base reaction. More interestingly, the dynamic imine bond and the neighborly thiophene can be converted into thieno[3,2-c]pyridine through an oxidative cyclization (Scheme 1). The thieno[3,2-c]pyridine as a new linkage was first reported in constructing COFs. The obtained COFs show ultrastability and good electron delocalization. Besides the conventional powder X-ray diffraction (PXRD) characterization analysis, high resolution TEM (HRTEM) clearly revealed the honeycomb-like internal structure of the COFs. Considering the advantages of stability and conjugation together with unique 2D structure, the photo-catalysis performance of the obtained COFs was further studied. Given the unique 2D molecular structure and the suitable band gap, the obtained COFs show great potential in photo-catalysis as a semiconductor material. Interestingly, slightly variation in the structure led to totally different photo-activity. **T-COF-2** containing triazine as the core exhibited the best NADH regeneration yield of 74% within 10 min which presents higher efficiency than most of the reported materials.

The building block **A** containing both thiophene and amine groups was synthesized via Suzuki coupling reaction. Two aldehyde building blocks **B** and **C** adopt benzene and triazine as cores, respectively. First, two imine-linked **COFs** were synthesized through the imine condensation reaction of

A+**B** and **A**+**C** in a mixture of 1, 2-dichlorobenzene/*n*-butanol/acetic acid under 120 °C for 3 days, giving crystalline yellow solids **B-COF-1** and **T-COF-1**, respectively. A reference compound **Ref-1** was also prepared by the same reaction between **A** and benzaldehyde. Further cyclization via Pictet-Spengler reaction between the β-carbon of the thiophene and the carbon of the imine gives the corresponding thieno[3,2-c]pyridine (**Ref-2**) in a yield of 89%. **B-COF-2** and **T-COF-2** were also prepared by the same reaction (For details see supporting information).

Scheme 1. Synthesis and structures of B-COF-1, 2; T-COF-1, 2; and Ref-1, 2.

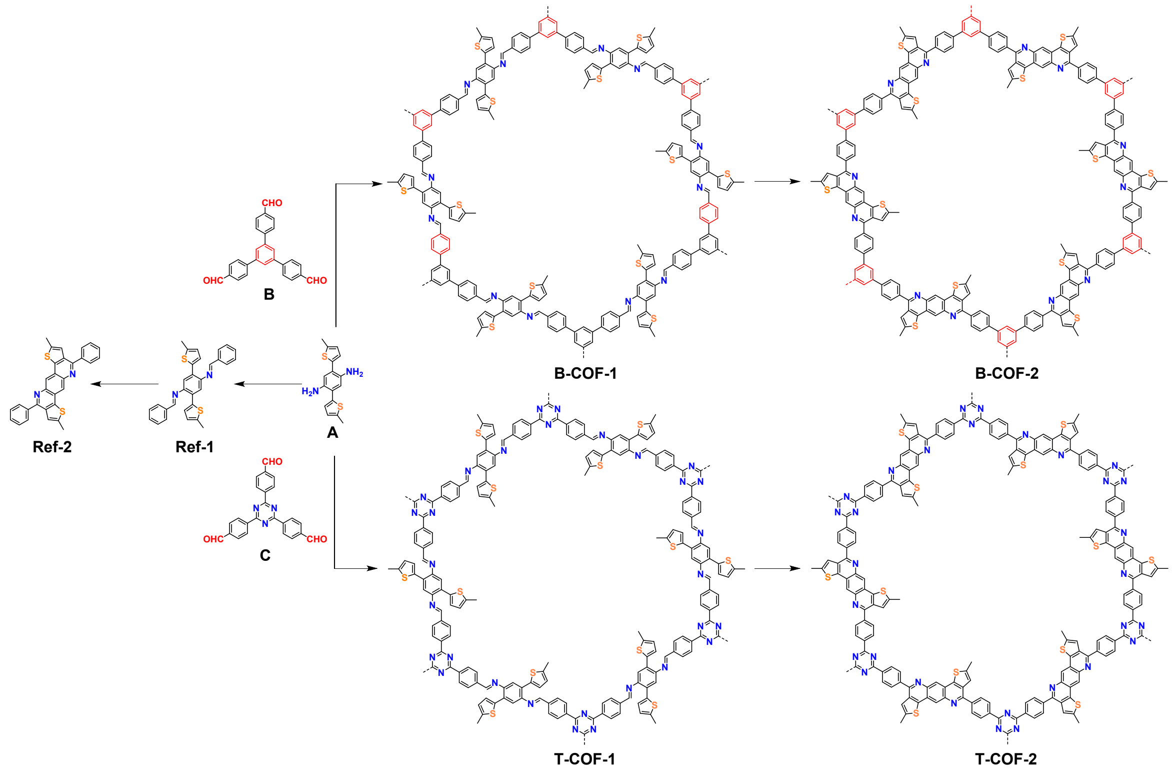

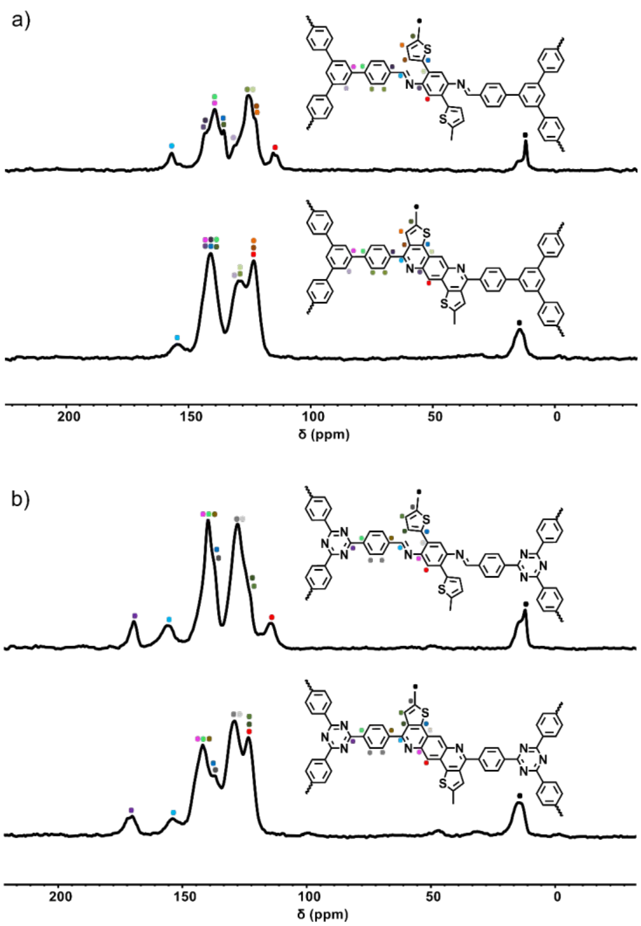

Figure 1. ^{13}C CP-MAS NMR spectra of **B-COF-1**, **2** (a) and **T-COF-1**, **2** (b).

To verify the chemical structures, the ^{13}C CP/MAS and FT-IR spectra of **B-COF-1, 2** and **T-COF-1, 2** were measured and compared, respectively. As depicted in Figure 1a-1b, the carbon peak of the C=N bond at about 157 ppm proved the existence of imine bonds in **B-COF-1** and **T-COF-1**. After acid catalyzed cyclization reaction, C=N bonds were supposed to become a part of the newly formed pyridine ring. Corresponding to the structural change, the carbon peak of the C=N bonds was found to move to 154 ppm in **B-COF-2** and **T-COF-2**. A similar change was also observed for **Ref-2** and **Ref-1**. Besides, the most obvious characteristic of the structural difference for **Ref-2** was found to be the carbon peak shift from 117 ppm to 123 ppm after cyclization. As expected, **B-COF-2** and **T-COF-2** entirely inherit the representative feature. The carbon peak at 115 ppm of **B-COF-1** and **T-COF-1** disappeared and a new peak at 123 ppm appeared in **B-COF-2** and **T-COF-2**. These significant changes indicated that the linkage was successfully converted into thieno[3,2-c]pyridine. FT-IR spectra also confirmed the conversion (Figure S1a-b). The C=N stretching modes characteristic of the imine were observed at about 1618 cm^{-1} for **B-COF-1** and **T-COF-1**. After cyclization, the signal displayed an obvious attenuation. Meanwhile, a new stretch signal appeared at about 1557 cm^{-1}. All the results above proved the formation of the imine bonds and the followed conversion of the linkages. Thermogravimetric analysis showed that the thieno[3,2-c]pyridine-linked COFs (**B-COF-2** and **T-COF-2**) possess better stability than their imine-linked precursor (**B-COF-1** and **T-COF-1**) with a decomposition temperature up to 460 °C (Figure S2).

The crystallinities of the materials were then evaluated by PXRD (Figure 2a-b). The four COFs all exhibit good crystallinities. Especially **B-COF-2** and **T-COF-2** are still highly crystalline after the cyclization reaction. No obvious shift of the prominent diffraction peaks was observed compared to the as-prepared imine-linked COFs, indicating the preservation of the highly ordered framework. The detailed structure information was given by comparison of the experimental PXRD profiles and the predicted profiles. As shown in Figure S3, the PXRD profiles calculated for AA stacking mode match excellently with the experimental profiles. **B-COF-1, 2** and **T-COF-1, 2** were concluded to be AA stacking. Furthermore, we performed nitrogen adsorption experiments to examine their porosities. The Brunauer-Emmett-Teller (BET) surface areas were observed to be 810 $m^2 g^{-1}$, 620 $m^2 g^{-1}$, 952 $m^2 g^{-1}$, 829 $m^2 g^{-1}$ for **B-COF-1, 2** and **T-COF-1, 2** respectively. The loss of the BET surface area after linkage conversion was attributed to the decrease of pore size and crystallinity. According to the pore size distribution data calculated by using non-local density functional theory (NLDFT) model, the pore size displayed an obvious reduction (Figure S4).

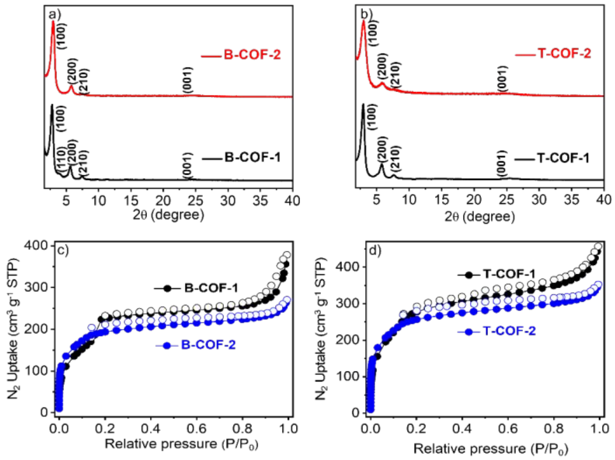

Figure 2. (a-b) The PXRD patterns of **B-COF-1**, **2** (a) and **T-COF-1**, **2** (b); (c-d) Nitrogen adsorption-desorption isotherms (77 K) of **B-COF-1**, **2** (c) and **T-COF-1**, **2** (d).

The chemical stability of converted COFs **B-COF-2** and **T-COF-2** were then examined. After submergence in HCl (12 M) or NaOH (12 M) solution at 50 °C for 24 hours, the crystallinities remain. No obvious differences were observed from the PXRD after the acid or base treatment (Figure S5), which demonstrates that the novel thieno[3,2-c]pyridine linkages in **B-COF-2** and **T-COF-2** bring excellent stability even under harsh conditions.

The periodic structural characteristics of **B-COF-2** and **T-COF-2** were also visualized by HRTEM. As shown in Figure 3, **B-COF-2** and **T-COF-2** displayed clear honeycomb-like porous structures. The HRTEM images combining with the corresponding Fast Fourier transformation (FFT) further confirmed the preservation of crystallinity and the structure. The bright spots indicate a center-to-center distance of the pore of ~2 nm in both **B-COF-2** and **T-COF-2**, which is in excellent agreement with the simulated structure model (2.3 nm, Figure S3). In sharp contrast, **B-COF-1** and **T-COF-1** are extremely unstable under the electron beam. HRTEM could not be obtained. These results further prove the excellent stability of converted COFs bring from the thieno[3,2-c]pyridine linkages.

As we know, nicotinamide adenine dinucleotide (NADH) as a typical coenzyme, whose regeneration process is the key step for solar energy utilization and biomass production since it plays an important role in various biochemical transformations.[50] Many materials have been applied for NADH regeneration. 80% of NADH regeneration yield can be obtained within 1hour by CdS-coated SiO_2 beads as the photocatalyst[51] TiO_2-CdS nanotubes can reach to 75.2% within 120 min.[50] The carbon nitride materials showed photo-regeneration yield of ~80 % in 45 min.[52] We recently reported a sp^2-carbon linked 2D COF with triazine as central units which give a 90% photo-regeneration yield in 12 mins.[42] Considering the fully conjugated structures, the COFs may act as good candidates for photocatalytic NADH regeneration. The photophysical properties of the COFs were measured first. According to the solid-state absorption spectra, obvious blue-shift occurred after the linkage conversion (Figure S7). Solid-state UV-vis measurements and cyclic voltammetry were performed to evaluate the band gap and LUMO energy level of **B-COF-2** and **T-COF-2**, respectively (Figure S7, S13). The band gaps of **T-COF-2** and **B-COF-2** are calculated to be 2.33 and 2.38 eV, respectively. Figure S13a shows the onset of reduction potential, from which the corresponding LUMO of **B-COF-2** was calculated to be -3.53 eV. A HOMO level of -5.91 eV was evaluated based on the optical band gap value. The LUMO and HOMO levels of **T-COF-2** were measured to be -3.50 and -5.83 eV. This electronic configuration suggests photo-activated COFs possess the thermodynamic driving force to reduce mediator to further transfer the hydride to the NAD^+.[54]

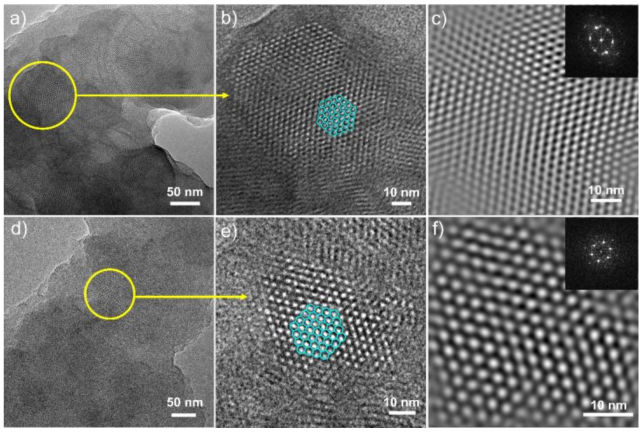

Figure 3. (a) TEM image of **B-COF-2**; (b) TEM image of **B-COF-2** enlarged view of a selected area in panel (a); (c) Fourier-filtered image of selected areas of **B-COF-2**, Inset: Fast Fourier Transform (FFT) from the selected areas; for **T-COF-2** see (d), (e), (f), respectively.

The photocatalysis performance for the regeneration of NADH was then evaluated. Here, the COFs materials play the role of collecting solar energy in the form of light-excited electrons. The electrons are then transferred to $[Cp^*Rh(bpy)(H_2O)]^{2+}$, followed by coupling with one proton to form the hydridehodium $[Cp^*Rh(bpy)(H)]^+$ (**M**, in abbreviation), which acts as a hydride transfer reagent towards NAD^+. In the end, the enzymatically active 1,4-NADH is exclusively generated (Figure S6). Subsequently, the solar energy was stored as the NADH which could activate various enzyme-mediated synthetic processes.[52] As shown in Figure 4, the peak at 340 nm is the characteristic absorbance peak of NADH which could indicate the regeneration efficiency of the NADH. The imine-linked **B-COF-1** showed no photoactivity at all, while **B-COF-2** displayed a regeneration yield of 5.5%. Interestingly, the NADH regeneration yield of **T-COF-2** displayed a dramatic increase compared with **T-COF-1**, reaching up to 74% in 10 min. This is a relatively high efficiency compared with most of other reported materials. Such obvious improvement of NADH regeneration efficiency arising from structure variation further demonstrated the successful conversion of linkages. The significant improvement of photoactivity could be ascribed to the extended conjugated structure which facilitates the electron delocalization. The photocurrent response was performed to indicate the separation efficiency of the photo-induced electron-hole pairs. As shown in Figure S12, Large enhancement of I_{ph} for **T-COF-2** was observed, indicating better separation of charged carriers than **B-COF-2**. In addition, according to the NADH regeneration yield of the different COFs, we could speculate that the nitrogen-rich triazine units brings a positive effect on photocatalysis. The free electron pair and the electron poor character may act as the active site for interface redox reaction.[53] In addition, **T-COF-2** can strongly bind with NAD^+ due to the π-π stacking interactions between the adenine subunit of NAD^+ and the π-conjugated 2D surface of **T-COF-2**. The charge transfer complex as a pre-state could facilite the photoinduced electron transfer between **T-COF-2** and NAD^+.[42] Similar phenomenon has also been found in the $g-C_3N_4$ as a photocatalast.[52, 55-56] To prove this proposal, a control experiment without

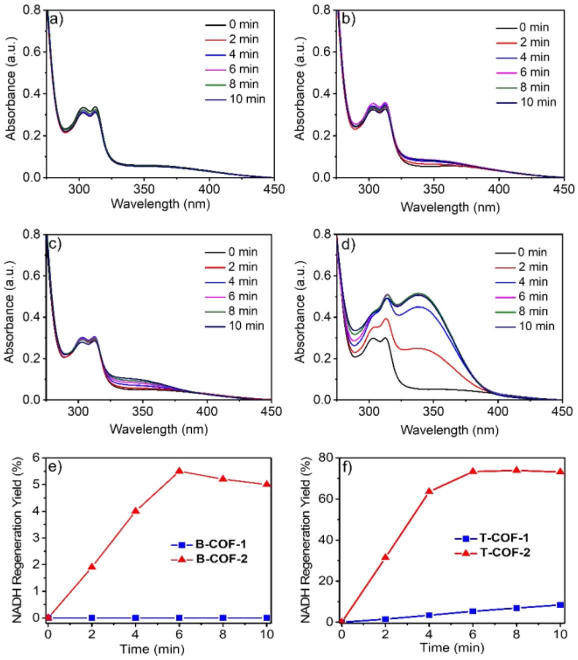

Figure 4. Experimental results of the NADH regeneration rates for **B-COF-1**, **2** and **T-COF-1**, **2**, respectively: (a-d) absorbance changes of NADH (e-f) photocatalytic NADH regeneration kinetics.

$[Cp^*Rh(bpy)(H)]^+$ was performed. The photoinduced electron transfer should in principle work without a further mediator ($[Cp^*Rh(bpy)(H)]^+$). As illustrated in Figure S9, without $[Cp^*Rh(bpy)(H)]^+$, NADH can still be moderately regenerated, the efficiency reach to 43.8% in 10 min. The photocatalytic stability of **T-COF-2** was then tested. As shown in Figure S10, no obvious decrease was observed after three cycles of the NADH regeneration experiment which indicated the excellent photo stability of **T-COF-2**.

In summary, we demonstrated the synthesis of two ultrastable fully π-conjugated thieno[3,2-c]pyridine-linked 2D COFs via a new two-steps synthetic strategy. This method allows the preservation of crystallinity and periodic frameworks. The semiconductor properties were also successfully improved after the linkage conversion. **B-COF-2** and **T-COF-2** exhibited NADH regeneration yield of 5.5% and 74.0% over 10 min, respectively, more efficient than the imine-linked precursor. The two-steps strategy provides a convenient method for the preparation of conjugated COFs and tuning of the semiconductor properties for photocatalysis.

ASSOCIATED CONTENT

Supporting Information

The Supporting Information is available free of charge on the ACS Publications website. Synthetic procedures, structural simulation, FT-IR, TGA, UV-Vis, NMR, including Figure S1-S16 (PDF).

AUTHOR INFORMATION

Corresponding Author

*yz@qust.edu.cn
*zbli@qust.edu.cn

Author Contributions

+Y.W. and H.L. contributed equally.

Notes

The authors declare no competing financial interests.

ACKNOWLEDGMENT

The work was supported by the National Natural Science Foundation of China (21905150), the National Young Thousand Talents Program, China Postdoctoral Science Foundation (2019M652338).

REFERENCES

(1) Fan, H.; Mundstock, A.; Feldhoff, A.; Knebel, A.; Gu, J.; Meng, H.; Caro, J., Covalent Organic Framework–Covalent Organic Framework Bilayer Membranes for Highly Selective Gas Separation. *J. Am. Chem. Soc.* **2018,** *140*, 10094-10098.

(2) Furukawa, H.; Yaghi, O. M., Storage of Hydrogen, Methane, and Carbon Dioxide in Highly Porous Covalent Organic Frameworks for Clean Energy Applications. *J. Am. Chem. Soc.* **2009,** *131*, 8875-8883.

(3) Gao, Q.; Li, X.; Ning, G.-H.; Xu, H.-S.; Liu, C.; Tian, B.; Tang, W.; Loh, K. P., Covalent Organic Framework with Frustrated Bonding Network for Enhanced Carbon Dioxide Storage. *Chem. Mater.* **2018,** *30*, 1762-1768.

(4) Kang, Z.; Peng, Y.; Qian, Y.; Yuan, D.; Addicoat, M. A.; Heine, T.; Hu, Z.; Tee, L.; Guo, Z.; Zhao, D., Mixed Matrix Membranes (MMMs) Comprising Exfoliated 2D Covalent Organic Frameworks (COFs) for Efficient CO_2 Separation. *Chem. Mater.* **2016,** *28*, 1277-1285.

(5) Li, Z.; Zhi, Y.; Feng, X.; Ding, X.; Zou, Y.; Liu, X.; Mu, Y., An Azine-Linked Covalent Organic Framework: Synthesis, Characterization and Efficient Gas Storage. *Chem. Eur. J.* **2015,** *21*, 12079-12084.

(6) Han, X.; Xia, Q.; Huang, J.; Liu, Y.; Tan, C.; Cui, Y., Chiral Covalent Organic Frameworks with High Chemical Stability for Heterogeneous Asymmetric Catalysis. *J. Am. Chem. Soc.* **2017,** *139*, 8693-8697.

(7) Lu, S.; Hu, Y.; Wan, S.; McCaffrey, R.; Jin, Y.; Gu, H.; Zhang, W., Synthesis of Ultrafine and Highly Dispersed Metal Nanoparticles Confined in a Thioether-Containing Covalent Organic Framework and Their Catalytic Applications. *J. Am. Chem. Soc.* **2017,** *139*, 17082-17088.

(8) Wei, P.-F.; Qi, M.-Z.; Wang, Z.-P.; Ding, S.-Y.; Yu, W.; Liu, Q.; Wang, L.-K.; Wang, H.-Z.; An, W.-K.; Wang, W., Benzoxazole-Linked Ultrastable Covalent Organic Frameworks for Photocatalysis. *J. Am. Chem. Soc.* **2018,** *140*, 4623-4631.

(9) Xu, H.; Gao, J.; Jiang, D., Stable, Crystalline, Porous, Covalent Organic Frameworks as A Platform for Chiral Organocatalysts. *Nat. Chem.* **2015,** *7*, 905-912.

(10) Ding, H.; Li, J.; Xie, G.; Lin, G.; Chen, R.; Peng, Z.; Yang, C.; Wang, B.; Sun, J.; Wang, C., An AIEgen-based 3D Covalent Organic Framework for White Light-emitting Diodes. *Nat. Commun.* **2018,** *9*, 5234.

(11) Haldar, S.; Chakraborty, D.; Roy, B.; Banappanavar, G.; Rinku, K.; Mullangi, D.; Hazra, P.; Kabra, D.; Vaidhyanathan, R., Anthracene-Resorcinol Derived Covalent Organic Framework as Flexible White Light Emitter. *J. Am. Chem. Soc.* **2018,** *140*, 13367-13374.

(12) Dalapati, S.; Jin, E.; Addicoat, M.; Heine, T.; Jiang, D., Highly Emissive Covalent Organic Frameworks. *J. Am. Chem. Soc.* **2016,** *138*, 5797-5800.

(13) Lin, G.; Ding, H.; Yuan, D.; Wang, B.; Wang, C., A Pyrene-Based, Fluorescent Three-Dimensional Covalent Organic Framework. *J. Am. Chem. Soc.* **2016,** *138*, 3302-3305.

(14) Li, H.; Chang, J.; Li, S.; Guan, X.; Li, D.; Li, C.; Tang, L.; Xue, M.; Yan, Y.; Valtchev, V.; Qiu, S.; Fang, Q., Three-Dimensional Tetrathiafulvalene-Based Covalent Organic Frameworks for Tunable Electrical Conductivity. *J. Am. Chem. Soc.* **2019,** *141*, 13324-13329.

(15) Li, X.; Gao, Q.; Wang, J.; Chen, Y.; Chen, Z. H.; Xu, H. S.; Tang, W.; Leng, K.; Ning, G. H.; Wu, J.; Xu, Q. H.; Quek, S. Y.; Lu, Y.; Loh, K. P., Tuneable Near White-emissive Two-dimensional Covalent Organic Frameworks. *Nat. Commun.* **2018,** *9*, 2335.

(16) Wu, X.; Han, X.; Xu, Q.; Liu, Y.; Yuan, C.; Yang, S.; Liu, Y.; Jiang, J.; Cui, Y., Chiral BINOL-Based Covalent Organic Frameworks for Enantioselective Sensing. *J. Am. Chem. Soc.* **2019,** *141*, 7081-7089.

(17) Liu, X.; Huang, D.; Lai, C.; Zeng, G.; Qin, L.; Wang, H.; Yi, H.; Li, B.; Liu, S.; Zhang, M.; Deng, R.; Fu, Y.; Li, L.; Xue, W.; Chen, S., Recent Advances in Covalent Organic Frameworks (COFs) as A Smart Sensing Material. *Chem. Soc. Rev.* **2019**, 48, 5266-5302.

(18) Ascherl, L.; Evans, E. W.; Gorman, J.; Orsborne, S.; Bessinger, D.; Bein, T.; Friend, R. H.; Auras, F., Perylene-Based Covalent Organic Frameworks for Acid Vapor Sensing. *J. Am. Chem. Soc.* **2019,** *141*, 15693-15699.

(19) Bessinger, D.; Ascherl, L.; Auras, F.; Bein, T., Spectrally Switchable Photodetection with Near-Infrared-Absorbing Covalent Organic Frameworks. *J. Am. Chem. Soc.* **2017,** *139*, 12035-12042.

(20) Lei, Z.; Yang, Q.; Xu, Y.; Guo, S.; Sun, W.; Liu, H.; Lv, L. P.; Zhang, Y.; Wang, Y., Boosting Lithium Storage in Covalent Organic Framework via Activation of 14-electron Redox Chemistry. *Nat. Commun.* **2018,** *9*, 576.

(21) DeBlase, C. R.; Silberstein, K. E.; Truong, T.-T.; Abruña, H. D.; Dichtel, W. R., β-Ketoenamine-Linked Covalent Organic Frameworks Capable of Pseudocapacitive Energy Storage. *J. Am. Chem. Soc.* **2013,** *135*, 16821-16824.

(22) Côté, A. P.; Benin, A. I.; Ockwig, N. W.; Keeffe, M.; Matzger, A. J.; Yaghi, O. M., Porous, Crystalline, Covalent Organic Frameworks. *Science* **2005,** *310*, 1166-1170.

(23) El-Kaderi, H. M.; Hunt, J. R.; Mendoza-Cortés, J. L.; Côté,

A. P.; Taylor, R. E.; Keeffe, M.; Yaghi, O. M., Designed Synthesis of 3D Covalent Organic Frameworks. *Science* **2007,** *316*, 268-272.

(24) Evans, A. M.; Parent, L. R.; Flanders, N. C.; Bisbey, R. P.; Vitaku, E.; Kirschner, M. S.; Schaller, R. D.; Chen, L. X.; Gianneschi, N. C.; Dichtel, W. R., Seeded Growth of Single-crystal Two-dimensional Covalent Organic Frameworks. *Science* **2018,** *361*, 52-57.

(25) Jackson, K. T.; Reich, T. E.; El-Kaderi, H. M., Targeted Synthesis of A Porous Borazine-linked Covalent Organic Framework. *Chem. Commun.* **2012,** *48*, 8823-8825.

(26) Roeser, J.; Prill, D.; Bojdys, M. J.; Fayon, P.; Trewin, A.; Fitch, A. N.; Schmidt, M. U.; Thomas, A., Anionic Silicate Organic Frameworks Constructed from Hexacoordinate Silicon Centres. *Nat. Chem.* **2017,** *9*, 977-982.

(27) Yahiaoui, O.; Fitch, A. N.; Hoffmann, F.; Fröba, M.; Thomas, A.; Roeser, J., 3D Anionic Silicate Covalent Organic Framework with srs Topology. *J. Am. Chem. Soc.* **2018,** *140*, 5330-5333.

(28) Keller, N.; Bessinger, D.; Reuter, S.; Calik, M.; Ascherl, L.; Hanusch, F. C.; Auras, F.; Bein, T., Oligothiophene-Bridged Conjugated Covalent Organic Frameworks. *J. Am. Chem. Soc.* **2017,** *139*, 8194-8199.

(29) Ma, J.-X.; Li, J.; Chen, Y.-F.; Ning, R.; Ao, Y.-F.; Liu, J.-M.; Sun, J.; Wang, D.-X.; Wang, Q.-Q., Cage Based Crystalline Covalent Organic Frameworks. *J. Am. Chem. Soc.* **2019,** *141*, 3843-3848.

(30) Pyles, D. A.; Crowe, J. W.; Baldwin, L. A.; McGrier, P. L., Synthesis of Benzobisoxazole-Linked Two-Dimensional Covalent Organic Frameworks and Their Carbon Dioxide Capture Properties. *ACS Macro Lett.* **2016,** 5, 1055-1058.

(31) Waller, P. J.; AlFaraj, Y. S.; Diercks, C. S.; Jarenwattananon, N. N.; Yaghi, O. M., Conversion of Imine to Oxazole and Thiazole Linkages in Covalent Organic Frameworks. *J. Am. Chem. Soc.* **2018,** *140*, 9099-9103.

(32) Seo, J. M.; Noh, H. J.; Jeong, H. Y.; Baek, J. B., Converting Unstable Imine-Linked Network into Stable Aromatic Benzoxazole-Linked One via Post-oxidative Cyclization. *J. Am. Chem. Soc.* **2019,** *141*, 11786-11790.

(33) Haase, F.; Troschke, E.; Savasci, G.; Banerjee, T.; Duppel, V.; Dorfler, S.; Grundei, M. M. J.; Burow, A. M.; Ochsenfeld, C.; Kaskel, S.; Lotsch, B. V., Topochemical Conversion of An Imine- into A Thiazole-linked Covalent Organic Framework Enabling Real Structure Analysis. *Nat. Commun.* **2018,** *9*, 2600.

(34) Acharjya, A.; Pachfule, P.; Roeser, J.; Schmitt, F.-J.; Thomas, A., Vinylene-Linked Covalent Organic Frameworks by Base-Catalyzed Aldol Condensation. *Angew .Chem. Int. Ed.* **2019,** *58*, 14865-14870.

(35) Xu, J.; He, Y.; Bi, S.; Wang, M.; Yang, P.; Wu, D.; Wang, J.; Zhang, F., An Olefin-Linked Covalent Organic Framework as a Flexible Thin-Film Electrode for a High-Performance Micro-Supercapacitor. *Angew .Chem. Int. Ed.* **2019,** *58*, 12065-12069.

(36) Lyu, H.; Diercks, C. S.; Zhu, C.; Yaghi, O. M., Porous Crystalline Olefin-Linked Covalent Organic Frameworks. *J. Am. Chem. Soc.* **2019,** *141*, 6848-6852.

(37) Jadhav, T.; Fang, Y.; Patterson, W.; Liu, C.-H.; Hamzehpoor, E.; Perepichka, D. F., 2D Poly(arylene vinylene) Covalent Organic Frameworks via Aldol Condensation of Trimethyltriazine. *Angew .Chem. Int. Ed.* **2019,** *58*, 13753-13757.

(38) Bi, S.; Yang, C.; Zhang, W.; Xu, J.; Liu, L.; Wu, D.; Wang, X.; Han, Y.; Liang, Q.; Zhang, F., Two-dimensional Semiconducting Covalent Organic Frameworks via Condensation at Arylmethyl Carbon Atoms. *Nat. Commun.* **2019,** *10*, 2467.

(39) Xu, S.; Wang, G.; Biswal, B. P.; Addicoat, M.; Paasch, S.; Sheng, W.; Zhuang, X.; Brunner, E.; Heine, T.; Berger, R.; Feng, X., A Nitrogen-Rich 2D sp^2-Carbon-Linked Conjugated Polymer Framework as a High-Performance Cathode for Lithium-Ion Batteries. *Angew .Chem. Int. Ed.* **2019,** *58*, 849-853.

(40) Jin, E.; Asada, M.; Xu, Q.; Dalapati, S.; Addicoat, M. A.; Brady, M. A.; Xu, H.; Nakamura, T.; Heine, T.; Chen, Q.; Jiang, D., Two-dimensional sp^2 Carbon-conjugated Covalent Organic Frameworks. *Science* **2017,** 357, 673-676.

(41) Chen, R.; Shi, J.-L.; Ma, Y.; Lin, G.; Lang, X.; Wang, C., Designed Synthesis of a 2D Porphyrin-Based sp^2 Carbon-Conjugated Covalent Organic Framework for Heterogeneous Photocatalysis. *Angew .Chem. Int. Ed.* **2019,** *58*, 6430-6434.

(42) Zhao, Y.; Liu, H.; Wu, C.; Zhang, Z.; Pan, Q.; Hu, F.; Wang, R.; Li, P.; Huang, X.; Li, Z., Fully Conjugated Two-Dimensional sp^2-Carbon Covalent Organic Frameworks as Artificial Photosystem I with High Efficiency. *Angew .Chem. Int. Ed.* **2019,** *58*, 5376-5381.

(43) Rao, M. R.; Fang, Y.; De Feyter, S.; Perepichka, D. F., Conjugated Covalent Organic Frameworks via Michael Addition-Elimination. *J. Am. Chem. Soc.* **2017,** *139*, 2421-2427.

(44) Guan, X.; Li, H.; Ma, Y.; Xue, M.; Fang, Q.; Yan, Y.; Valtchev, V.; Qiu, S., Chemically Stable Polyarylether-based Covalent Organic Frameworks. *Nat. Chem.* **2019,** *11*, 587-594.

(45) Guo, J.; Xu, Y.; Jin, S.; Chen, L.; Kaji, T.; Honsho, Y.; Addicoat, M. A.; Kim, J.; Saeki, A.; Ihee, H.; Seki, S.; Irle, S.; Hiramoto, M.; Gao, J.; Jiang, D., Conjugated Organic Framework with Three-dimensionally Ordered Stable Structure and Delocalized pi Clouds. *Nat. Commun.* **2013,** *4*, 2736.

(46) Wang, M.; Ballabio, M.; Wang, M.; Lin, H.-H.; Biswal, B. P.; Han, X.; Paasch, S.; Brunner, E.; Liu, P.; Chen, M.; Bonn, M.; Heine, T.; Zhou, S.; Cánovas, E.; Dong, R.; Feng, X., Unveiling Electronic Properties in Metal-Phthalocyanine-Based Pyrazine-Linked Conjugated Two-Dimensional Covalent Organic Frameworks. *J. Am. Chem. Soc.* **2019,** *141*, 16810-16816.

(47) Zhang, B.; Wei, M.; Mao, H.; Pei, X.; Alshmimri, S. A.; Reimer, J. A.; Yaghi, O. M., Crystalline Dioxin-Linked Covalent Organic Frameworks from Irreversible Reactions. *J. Am. Chem. Soc.* **2018,** *140*, 12715-12719.

(48) Wang, P.-L.; Ding, S.-Y.; Zhang, Z.-C.; Wang, Z.-P.; Wang, W., Constructing Robust Covalent Organic Frameworks via Multicomponent Reactions. *J. Am. Chem. Soc.* **2019,** *141*, 18004-18008.

(49) Li, X.; Zhang, C.; Cai, S.; Lei, X.; Altoe, V.; Hong, F.; Urban, J. J.; Ciston, J.; Chan, E. M.; Liu, Y., Facile Transformation of Imine Covalent Organic Frameworks into Ultrastable Crystalline Porous Aromatic Frameworks. *Nat. Commun.* **2018,** *9*, 2998.

(50) Ryu, J.; Lee, S. H.; Nam, D. H.; Park, C. B., Rational Design and Engineering of Quantum-dot-sensitized TiO_2 Nanotube Arrays for Artificial Photosynthesis. *Adv. Mater.* **2011,** *23*, 1883-1888.

(51) Lee, S. H.; Ryu, J.; Nam, D. H.; Park, C. B., Photoenzymatic Synthesis through Sustainable NADH Regeneration by SiO_2-supported Quantum Dots. *Chem. Commun.* **2011,** *47*, 4643-4645.

(52) Liu, J.; Antonietti, M., Bio-inspired NADH Regeneration by Carbon Nitride Photocatalysis using Diatom Templates. *Energy Environ. Sci* **2013,** *6*, 1486-1493.

(53) Zhang, G.; Lan, Z. A.; Wang, X., Conjugated Polymers: Catalysts for Photocatalytic Hydrogen Evolution. *Angew .Chem. Int. Ed.* **2016,** 55, 15712-15727.

(54) Steckhan, E.; Herrmann, S.; Ruppert, R.; Dietz, E.; Frede, M.; Spika, E., Analytical Study of A Series of Substituted (2,2'-bipyridyl)(pentamethylcyclopentadienyl)rhodium and -iridium Complexes with Regard to Their Effectiveness as Redox Catalysts for the Indirect Electrochemical and Chemical Reduction of NAD(P)+. *Organometallics* **1991,** 10, 1568-1577.

(55) Liu, J.; Huang, J.; Zhou, H.; Antonietti, M., Uniform Graphitic Carbon Nitride Nanorod for Efficient Photocatalytic Hydrogen Evolution and Sustained Photoenzymatic Catalysis. *ACS Appl. Mater. Interfaces* **2014,** 6, 8434-8440.

(56) Huang, J.; Antonietti, M.; Liu, J, Bio-inspired Carbon Nitride Mesoporous Spheres for Artificial Photosynthesis: Photocatalytic Cofactor Regeneration for Sustainable Enzymatic Synthesis. *J. Mater. Chem. A.* **2014,** 2,7686-7693.

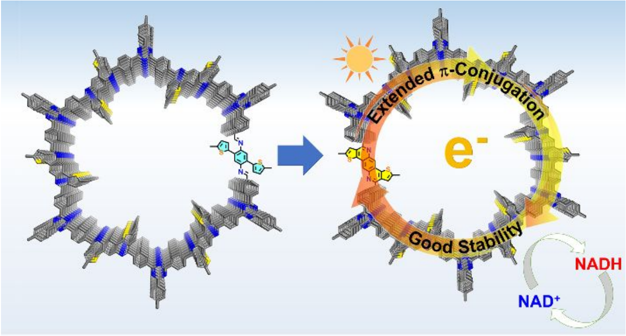
Extended π-Conjugation
e⁻
Good Stability
NADH
NAD⁺